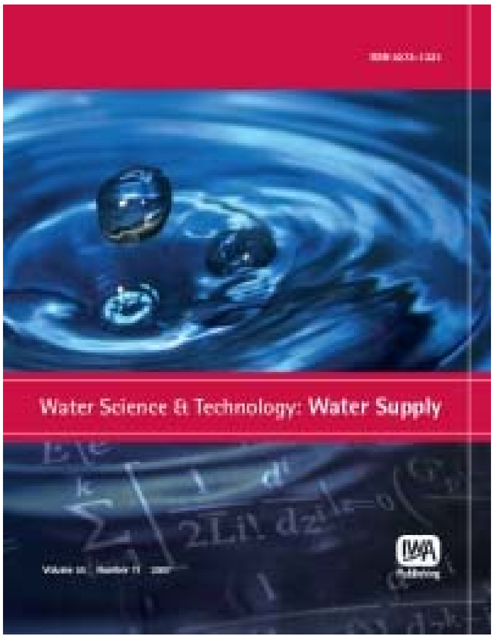
Water Science & Technology: Water Supply

Influence of pyrolytic seeds on ZnO nanorod growth onto rigid substrates for photocatalytic abatement of *Escherichia coli* in water

Luis Sanchez, Lucas Guz, Pilar García, Silvia Ponce, Silvia Goyanes, María Claudia Marchi, Roberto Candal, Walter Estrada and Juan Rodriguez

ABSTRACT

ZnO nanorods (ZnO NRs) were grown on ZnO seeded fluorine doped tin oxide (FTO) substrates at low temperatures (90 °C) from Zn^{2+} precursors in alkaline aqueous solution. The ZnO seeds were deposited on the FTO substrate heated at 350 °C by spray pyrolysis of a zinc acetate solution in a water ethanol mixture. The structure of seeds was tuned by the ethanol water ratio, Γ, which controls the solvent evaporation rate of drops impinging the substrate. The relationship between the microstructure and optical properties of the ZnO NR films and the photocatalytic antibacterial activity for *Escherichia coli* abatement, was determined through a detailed characterization of the material. The higher photocatalytic antibacterial activity was performed by ZnO NR films grown on seeds deposited from solutions with Γ in the 0.0–0.03 range. With these films, the population of viable *E. coli* dropped more than six orders, from 8×10^8 to 4×10^2 CFU. These results show the potential of these materials in water disinfection.

Key words | nanorods, photocatalytic disinfection, spray pyrolysis, ZnO

Luis Sanchez
Pilar García
Walter Estrada
Juan Rodriguez (corresponding author)
Universidad Nacional de Ingeniería,
Lima, Perú
E-mail: *jrodriguez@uni.edu.pe*

Lucas Guz
Roberto Candal
Escuela de Ciencia y Tecnología,
Universidad Nacional de San Martín,
Argentina

Silvia Ponce
University of Lima,
Lima, Perú

Silvia Goyanes
Departamento de Física,
FCEyN, Universidad de Buenos Aires,
IFIBA-CONICET,
Argentina

María Claudia Marchi
Roberto Candal
INQUIMAE, FCEyN, Universidad de Buenos Aires,
Argentina

INTRODUCTION

New promising processes for water disinfection based on heterogeneous photocatalysis with nanostructured semiconductors are currently under development (Hua *et al.* 2012), because of being able to oxidize low concentrations of organic pollutants into benign products (Chen *et al.* 2012; Wang *et al.* 2012). Zinc oxide (ZnO) is an important semiconductor material with a direct wide bandgap (3.37 eV) at room temperature. ZnO is considered a promising candidate for photocatalysis applications, owing to its bandgap value and a rich family of nanostructures (Wang 2004), such as nanotubes (Luo *et al.* 2010), nanowires (Elias *et al.* 2008) and nanorods (Hari *et al.* 2008), which present different charge transport properties than spheroidal nanoparticles, higher surface-to-volume ratio and strengthen contacts with the organic material, resulting in the enhanced photocatalytic efficiency (Wang *et al.* 2008). ZnO was recently reported as a photocatalytic material to inactivate Gram-negative bacteria *Escherichia coli* (Rodríguez *et al.* 2010; Alarcón *et al.* 2011); and Gram-positive bacteria such as *Lactobacillus helveticus* (Liu & Yang 2003) and *Staphylococcus aureus* (Jaisai *et al.* 2012; Talebian *et al.* 2013). Most of the studies reported in the literature use ZnO powders from different sources and with different shapes. Recently, Talebian *et al.* (2013) demonstrated that the shape of the ZnO particles has an important effect on antibacterial activity, flower like particles being very active, followed by rods and spheres, and Baruah *et al.* (2012) reported the development of a portable device for water purification that used ZnO-NRs attached

doi: 10.2166/ws.2014.068

to polyethylene fibers as a photocatalyst with antibacterial activity. ZnO nanorods (ZnO NRs) present the advantage that they can be grown onto different substrates, e.g. glass, quartz, conductive glass, silicon, paper and plastics using wet chemistry such as sol–gel or hydrothermal processes, provided the substrate is suitably seeded. Moreover, it has been demonstrated that the presence of seeds is a necessary condition for obtaining arrays of oriented supported ZnO NRs, otherwise deposits are formed by diverse structures – e.g. flowers and stars grown from a nucleus developed in the solution phase (Yi *et al.* 2007; Ma *et al.* 2011). Zinc acetate alcoholic solutions have proven to be suitable precursors for ZnO seeds (Byrne *et al.* 2010). Typically, the solution is deposited on the substrate by dip-coating or drop coating followed by annealing, or by spray pyrolysis (SP). Both methods require heating of the substrate at temperatures close to 350 °C to produce the seeds. Recently, the influence of the seeds in the morphology of the obtained ZnO NRs was reported (Rodríguez *et al.* 2013), however, up to now, there is not in the literature a systematic study of the influence of the seeds on the photocatalytic ability of the material to disinfect water. This knowledge is necessary for the development of versatile and stable devices with capacity for the purification of large volumes of water. In this work we will evaluate the influence of the depositing seed parameters by the SP technique on the rod morphology and the photocatalytic degradation of *E. coli* bacteria in water.

MATERIAL AND METHODS

The chemical reactants used as precursors for ZnO seeds and rods were, respectively, analytical grade zinc acetate [$Zn(CH_3COO)_2$. $6H_2O$] and zinc nitrate [$Zn(NO_3)_2.6H_2O$] pro analysis (PA) 100% from Fermont. Sodium hydroxide (NaOH) 98% PA, from EKA Chemicals was used for the nanorods growth solution.

Conductive glass (fluorine doped tin oxide (FTO), Libbey Owens Ford glass substrates coated with a layer of transparent and conducting SnO_2:F having a resistance of 8 Ω/cm^2) was used as the substrate for the growth of ZnO nanorods; $2.0 \times 1.5\ cm^2$ pieces of FTO conductive glass were cleaned in an ultrasonic bath, first with water and then with ethanol, before depositing the seed layer.

Seed deposition

Zinc oxide seed films were first deposited onto the precleaned FTO-coated glass substrate using SP technique (Quintana *et al.* 2002) and were then subsequently used as the substrate to grow ZnO nanorods.

In a homemade SP device described in detail elsewhere (Quintana *et al.* 2005) a medical nebulizer was used as atomizer to produce uniform size droplets which were directed by a nozzle towards the hot substrate (350 °C). The nozzle performed an oscillating movement at constant velocity to scan the whole area of the substrate. The precursor used in all experiments for the present work was a 0.10 mol/L zinc acetate solution in a mixture of deionized water and ethanol. The molar ethanol/water ratio (Γ) was varied within the range 0 to 0.92. Some drops of acetic acid were added to ensure both the total dissolution of zinc acetate and to adjust the pH to 5.8. Micro-filtered air was used as a carrier gas at a fixed pressure of 1.7×10^5 Pa and maintained at a constant flux of 15 L/min. Compared to previous works where thick films of ZnO were grown (typically several hundreds of nm obtained for 60 min of deposition time) (Quintana *et al.* 2005), in the present case, thin layers (typically less than 100 nm) of ZnO were used as seeds for the growth of the NRs. Typically, this represented about 10 sweeps of our SP setup for the deposition of the seeds obtained for about one minute of deposition time (Rodríguez *et al.* 2010).

Growth of ZnO NR films

The solution medium used for the growth of the ZnO NRs was prepared as follows: equal volumes of $Zn(NO_3)_2.6H_2O$ (0.15 mol/L) and NaOH (2.1 mol/L) were mixed under continuous stirring. A white precipitate was formed approximately one minute after mixing. The complete system was aged overnight at 23 °C and filtered under vacuum to obtain a clear solution.

The substrates seeded with ZnO films were placed in a 100 mL screw-capped glass flask (Normax) and the solution medium for the growth of ZnO NRs was added. This glass flask containing the substrate and the solution was placed in an oven at 90 °C for 1 h. These parameters were selected in order that ZnO NRs growth occurred in the regime of slow kinetics (Guo *et al.* 2005). The morphology and the structure of the NRs depend on the characteristics of the ZnO seeds, as will be discussed below. The substrates covered with ZnO NRs (FTO/ZnO NRs) were then removed from the solution, cleaned with water, ethanol and dried at 60 °C.

Measurement of photocatalytic activity

The reactor system used to study the photocatalytic efficiency of the synthesized materials on the degradation of bacteria *E. coli* ATCC 25,922 is shown in Figure 1(a). The light source was an Ultravitalux 220 W OSRAM lamp, placed approximately 30 cm above the cylindrical photoreactor. The precise lamp to sample distance was set in order to obtain an incident radiation intensity of 30 W/m^2 in the UV A/B light range; measured with an UV Light Meter model YK-34 UV. Figure 1(b) shows the emission spectra of the OSRAM lamp, determined with an Ocean Optics USB 4,000 spectrometer.

An aqueous solution with initial volume of 50 mL was prepared with a bacteria concentration of about 10^9 CFU/ml and placed in the photoreactor. Samples of FTO/ZnO NRs, 2.0 × 1.5 cm^2, were immersed facing the light, then 1 mL of solution was collected at different intervals of time (0, 30, 60 and 90 min). Samples were diluted 1:10 with double-distilled water in order to obtain a solution containing CFU in the range: 10–500 CFU/ml. Then 1 mL of the final dilution was taken and vacuum filtered through a sterile filter. This results in all bacteria present in the water being retained on the filter. Finally, the filter was placed onto a paper pad soaked in a liquid growth medium (Membrane lauryl sulfate broth (Oxoid MM0615)), which feeds *E. coli* bacteria, but inhibits the growth of any other bacteria on the filter. Finally the concentration of bacteria was determined by counting, after incubating at 40 °C for 16 h.

RESULTS AND DISCUSSION

Influence of the ethanol to water molar ratio of the seed precursor solution on the diameters of the NRs

The morphology of films and NRs was studied using scanning electron microscopy (SEM) with an ULTRA-55 field emission SEM (Carl Zeiss SMT AG) working at an electron beam energy of 15 keV. Analysis of the rod size distribution was made with the ImageJ software (http://rsb.info.nih.gov/ij/). Figure 2(a) shows SEM images of typical ZnO NRs grown over seeds deposited by SP using precursor solutions with an ethanol/water ratio of $\Gamma = 0.00$. The distribution of ZnO NRs diameters is shown in Figure 2(b). All NRs displayed a hexagonal cross section and grew almost perpendicularly oriented to the surface, as can be seen in the cross section and magnified image shown in Figures 2(c) and 2(d) respectively. We performed similar measurements for the samples grown from seeds for various intermediate ethanol/water ratios Γ, from $\Gamma = 0.0$ to $\Gamma = 0.92$, and for each sample we extracted from the SEM images the distribution of diameters of the NRs. The results are

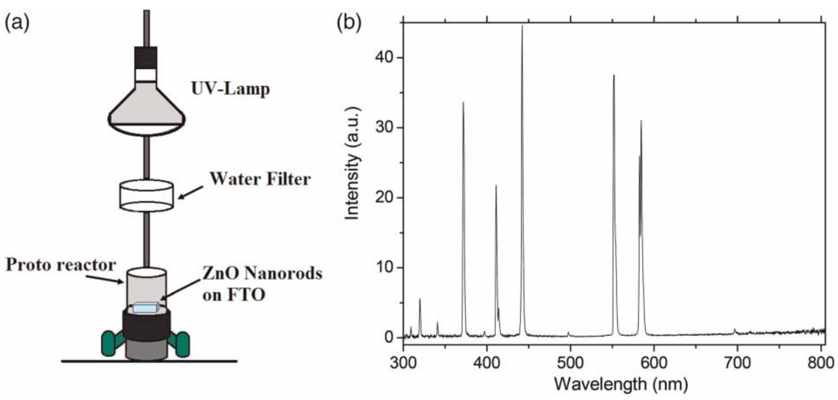

Figure 1 | (a) Photocatalytic reactor system for degradation with UV lamp and (b) emission spectra of the OSRAM lamp.

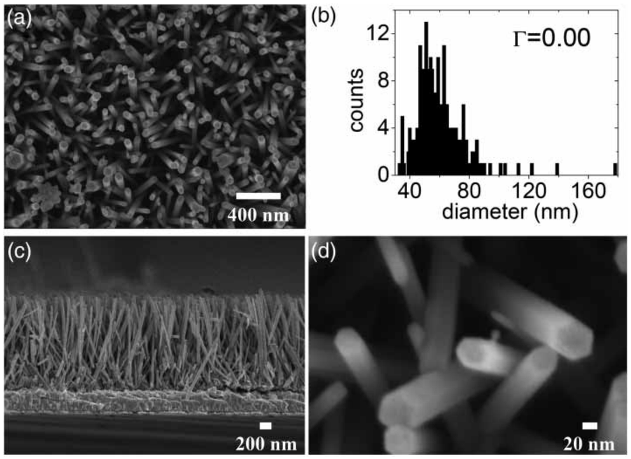

Figure 2 | (a) Typical SEM image of ZnO nanorods grown on FTO substrates with ZnO seeds obtained for an ethanol to water molar ratio $\Gamma = 0.00$, (b) histogram of the distribution of diameters for the obtained ZnO NRs as measured from the SEM images, (c) SEM images of cross section, (d) higher magnification top-view of NR films grown on FTO.

summarized in Table 1. Both the average diameter and their dispersion exhibit a trend to a minimum for Γ in the range 0.02 to 0.06.

Figure 3 shows the number of rods per unit of area counted on two different magnification sets of SEM images. It is observed that for both sets of analysis, 0.17 and 0.73 μm^2, respectively, the NR density presents a maximum around $\Gamma = 0.03$.

The calculated surface area A_s of NRs, was calculated considering a rod as a hexagonal prism, for the same areas of analysis mentioned before; the results are show in Figure 4. In both cases the increment of the surface active area is between 48 to 58 times higher than the area of a flat surface.

Crystallinity and orientation

The crystalline structure of the NRs was determined by X-ray diffraction analysis, the results are shown in Figure 5. The diffraction patterns correspond to the hexagonal wurtzite structure of ZnO. For each sample, peaks corresponding to (002), (101), (102) and (103) planes are clearly seen, with the (002) peak dominating, which indicates that the *c*-axis of the wurtzite structure is the preferential direction of growth of the NRs, as usually observed for ZnO NRs. The crystallite size along the *c*-axis can be estimated for each sample from the full-width-at-half-maximum (FWHM) of the (002) line using Debye–Scherrer's equation, that is, $D = 0.9\lambda/\beta \cos\theta$ where $\lambda = 1.540{,}598$ Å is the wavelength of the CuKα radiation, θ the diffraction angle and β is the FWHM of the (002) diffraction peak. The calculated crystalline domain size is about 12 to 14 nm, regardless of the value of Γ, as can be seen in Table 1.

Absorbance in the UV-vis-NIR

Specular transmittance spectra (*Ts*) for ZnO NR arrays were recorded in the $300 < \lambda < 1{,}000$ nm range with a UV-vis spectrophotometer (Agilent 8453). In general, the transmittance is below 68% for wavelengths in the near-infrared (NIR) (see Table 1 and Figure 6). From the transmittance measurements and using the film thicknesses as obtained by SEM cross section measurements (Table 1), and considering

Table 1 | Summary of parameters obtained for ZnO NR films, (a) thickness estimated from cross sectional SEM pictures, (b) average NR diameter derived from SEM images, (c) grain size calculated from Scherrer's equation, (d) optical transmittance at 550 nm from UV-vis spectra and (e) optical bandgap obtained from Figure 6

Sample	(a) Sample thickness (nm)	(b) Average diameter of the NRs (nm)	(c) Grain size (nm)	(d) Transmittance at 550 nm (%)	(e) Optical bandgap E_g (eV)
Bare FTO	346 ± 5			84.3	
$\Gamma = 0$	1600 ± 40	54 ± 17	12.6	17.3	3.1 ± 0,05
$\Gamma = 0.03$	1750 ± 50	51 ± 20	12.8	14.1	3.15 ± 0,05
$\Gamma = 0.04$	1620 ± 50	43 ± 14	12.2	33.6	3.20 ± 0,05
$\Gamma = 0.06$	1730 ± 80	49 ± 19	12.2	22.5	3.20 ± 0,05
$\Gamma = 0.31$	1050 ± 25	59 ± 29	13.0	11.3	2.8 ± 0,05
$\Gamma = 0.92$	1530 ± 50	67 ± 37	12.8	9.2	2.9 ± 0,05

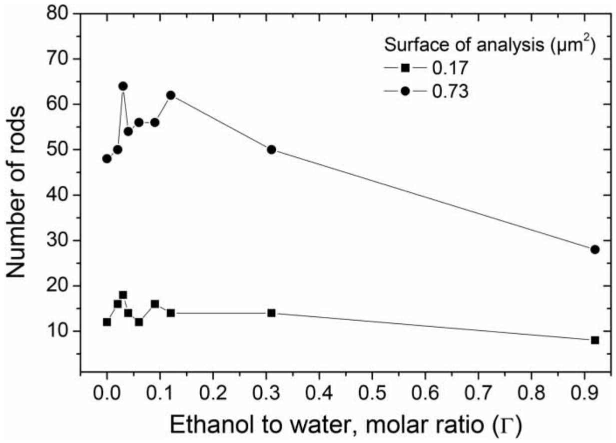

Figure 3 | Nanorod surface density obtained from seeds fabricated using different ethanol–water molar ratios Γ for the initial seeding conditions.

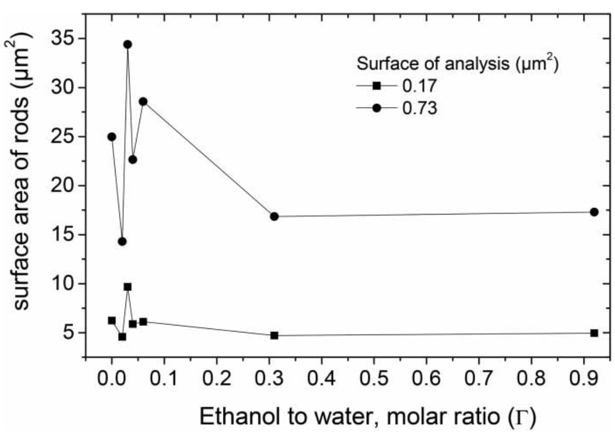

Figure 4 | Surface area of rods obtained from seeds fabricated using different ethanol–water molar ratios Γ for the initial seeding conditions.

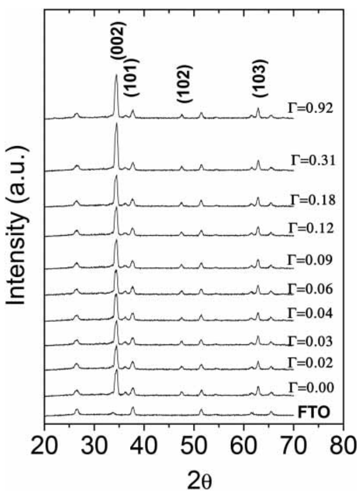

Figure 5 | X-ray diffraction pattern of ZnO NRs grown on FTO substrates seeded by SP at Γ values shown in the figure.

direct optical transitions, the direct bandgap, E_g can be estimated from the following empirical formula:

$$\alpha h\nu = A\sqrt{E - E_g} \quad (1)$$

In this formula, A is a constant, E_g is the optical bandgap, α is the absorption coefficient and E is the photon energy which can be converted to a wavelength using the relation E (eV) $= 1240/\lambda$(nm). The absorption coefficient α can be estimated from the normalized transmittance T using the equation

$$T = e^{-\alpha d} \quad (2)$$

where d is the thickness of the samples. The extrapolation of a linear part of the curve $(\alpha E)^2$ *vs* E to 0 as shown in Figure 6 allows us to obtain the optical bandgap (E_g) of the sample. The results of this analysis for the different samples grown at different seeding conditions Γ are summarized in Table 1. The extrapolated optical bandgap for direct transitions (Ahn *et al.* 2008) presents a noticeable change as a function of Γ with a maximum obtained for $\Gamma = 0.03$–0.06, which correlates with the NR samples having a thinner diameter.

Effect of ethanol water ratio, Γ, on the photocatalytic antibacterial activity

The ZnO NRs synthesized onto a glass substrate were used for the photocatalytic inactivation of *E. coli* bacteria

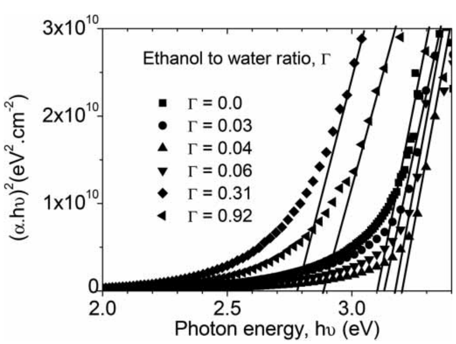

Figure 6 | Absorption spectra for ZnO NR samples grown using different ethanol–water molar ratios Γ for the initial seeding conditions. The straight lines correspond to extrapolation of the linear parts of the spectra in order to extract the bandgap energy E_g.

in water. The results are shown in Figure 7. Illumination using 30 W/m^2 in the UV-A/-B range was selected due to its nil influence in reducing the bacterial population (photolysis plot). Clearly, in the dark (without illumination), there was no influence of the ZnO nanorods on the viability of bacteria. When the ZnO NRs films in water were irradiated with the same UV illumination, an effective photocatalytic degradation of the bacteria in water was observed. As can be seen in Figure 7, ZnO NRs synthetized from seeds pyrolytically deposited at the ethanol to water molar ratio in the $\Gamma = 0–0.03$ range possessed the best antibacterial activities. These results correlate well with the NR samples having thinner diameter and higher exposed surface area. This fact is in agreement with the trend observed in Figures 3 and 4, in which ZnO NRs prepared from a seed layer deposited using ethanol/water precursor solutions in the range $\Gamma = 0.0–0.03$ presented a larger density of NRs as well as a larger available surface to drive photocatalytic experiments. The higher activity was displayed by the samples seeded using solutions with $\Gamma = 0.03$, which presented the higher area and UVA absorbance. Although the experiments were not performed until total disinfection, the reduction of the viable population of *E. coli* was more than six orders, from 8×10^8 to 4×10^2 CFU/mL. Total disinfection was not accomplished because the initial bacteria concentration was very high in order to test the performance and resistance against fooling of the photocatalyst. However, the remarkable reduction in viable *E. coli* indicates that this material is very promissory for

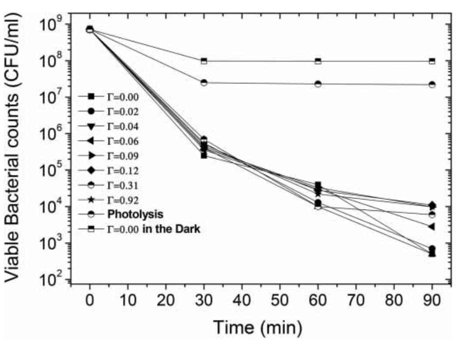

Figure 7 | *E. coli* degradation under UV-irradiated ZnO nanorod films in water. The plot corresponds to the photocatalytic experiments performed with ZnO NR growth onto seeds pyrolytically deposited at the ethanol–water molar ratio Γ.

application in water disinfection, even in water with high concentration of microorganism. Other authors reported total disinfection with powder and supported ZnO, albeit starting with a much lower concentration of *E. coli* (see for example Baruah *et al.* (2012) and Talebian *et al.* (2013)).

Samples before and after the photocatalytic experiments were analyzed by SEM and the results are shown in Figure 8. As a general trend, no changes were observed between samples before and after the photocatalytic experiments. In addition it is interesting to remark that in all the cases, the remains of bacteria photocatalytically degraded were presented on the surface of the ZnO NR films. Long term experiments are currently under development in order to test the mechanical stability of the ZnO NR films, as well as the effect of the photocatalyzed bacteria on the catalyst efficiency.

CONCLUSIONS

ZnO NR films, with high surface area and photocatalytic activities under UV irradiation, were synthesized by hydrothermal treatment. We demonstrated that the nature of the ZnO seeds have a strong influence on the characteristics of the ZnO NR films and on their antibacterial activity. SP seeded films led to NRs whose diameters were dependent on the ethanol to water molar ratio (Γ) in the precursor solution. Consequently, the active surface area of the obtained ZnO NRs was dependent on Γ. The highest area was obtained for Γ in the range 0.0–0.03. The NR films displayed effective photocatalytic disinfection activity on *E. coli* in water. ZnO NRs synthesized from seeds pyrolytically deposited at the ethanol to water molar ratio in the $\Gamma = 0.00$ to 0.03 range possess the best antibacterial activities, which correlates with the NR samples having a thinner diameter, larger number of rods per unit area and larger surface area of rods. The concentration of viable *E. coli* dropped more than six orders and the films of ZnO NRs were not notably modified after the photocatalytic treatment. These facts indicate that this material is very promising for the development of devices for water purification.

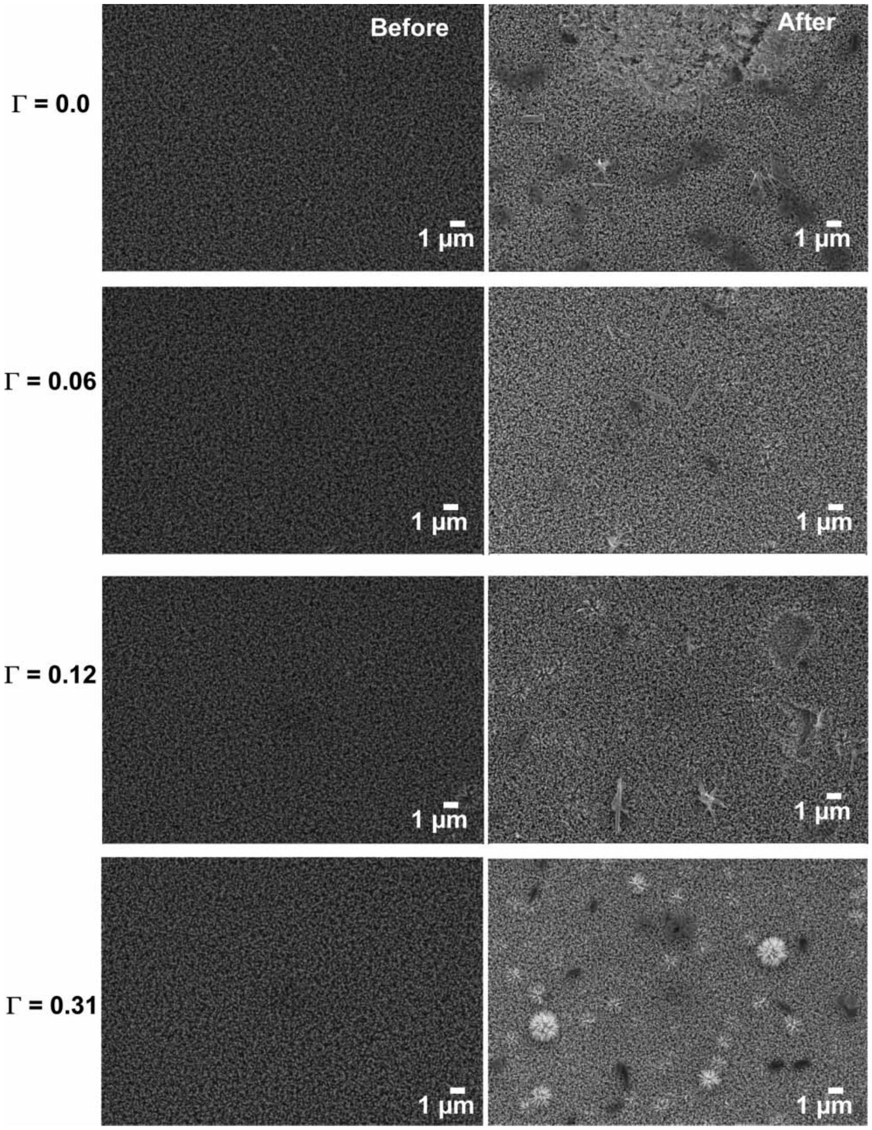

Figure 8 | SEM images of ZnO nanorods grown on FTO substrates with ZnO seeds obtained at he shown ratio ethanol to water molar ratio Γ before (a) and after (b) of the photocatalytic disinfection experiment.

ACKNOWLEDGEMENTS

This work was supported by the Fincyt Project (Contract No140-FINCYT-IB-2013), Concytec-403–2012 OAJ Project, Peruvian-Argentinean 2011–02-CONCYTEC OAJ Project and MINCYT-CONCYTEC PE/11/02, CONICET-PIP 112–200801–02533, UBACyT 20020090100297 and ANPCyT PICT 1093. RC, MCM and SG are members of CONICET. The CONICET fellowship granted to LG is acknowledged.

REFERENCES

Ahn, K., Shet, S., Deutsch, T., Jiang, C., Yan, Y., Al-Jassim, M. & Turner, J. 2008 Enhancement of photoelectrochemical response by aligned nanorods in ZnO thin films. *Journal of Power Sources* **176**, 387–392.

Alarcón, J., Ponce, S., Paraguay Delgado, F. & Rodriguez, J. 2011 Effect of γ-irradiation on the growth of ZnO nanorod films for photocatalytic disinfection of contaminated water. *Journal of Colloid and Interface Science* **364**, 49–55.

Baruah, S., Jaisaia, M. & Dutta, J. 2012 Development of a visible light active photocatalytic portable water purification unit using ZnO nanorods. *Catalysts Science and Technology* **2**, 918–921.

Byrne, D., McGlynn, E., Henry, M. O., Kumar, K. & Hughes, G. 2010 A novel, substrate independent three-step process for the growth of uniform ZnO nanorod arrays. *Thin Solid Films* **518**, 4489–4492.

Chen, H., Nanayakkara, C. & Grassian, V. 2012 Titanium dioxide photocatalysis in atmospheric chemistry. *Chemical Reviews* **112**, 5919–5948.

Elias, J., Tena-Zaera, R. & Lévy-Clément, C. 2008 Electrochemical deposition of ZnO nanowire arrays with tailored dimensions. *Journal of Electroanalytical Chemistry* **621**, 171–177.

Guo, M., Peng, D. & Shengmin, C. 2005 Hydrothermal growth of well-aligned ZnO nanorod arrays: Dependence of morphology and alignment ordering upon preparing conditions. *Journal of Solid State Chemistry* **178**, 1864–1873.

Hari, P., Baumer, M., Tennyson, W. D. & Bumm, L. A. 2008 ZnO nanorod growth by chemical bath method. *Journal of Non-Crystalline Solids* **354**, 2843–2848.

Hua, T., Ouyang, S., Bi, Yi., Umezawa, Na., Oshikiri, M. & Ye, J. 2012 Nano-photocatalytic materials: possibilities and challenges. *Advanced Materials* **24**, 229–251.

Jaisai, M., Baruah, S. & Dutta, J. 2012 Paper modified with ZnO nanorods – antimicrobial studies. *Beilstein Journal of Nanotechnology* **3**, 684–691.

Liu, H. L. & Yang, C. K. 2003 Photocatalytic inactivation of *Escherichia coli* and *Lactobacillus helveticus* by ZnO and TiO_2 activated with ultraviolet light. *Process Biochemistry* **39**, 475–481.

Luo, L., Lv, G., Li, B., Hu, X., Jin, L., Wang, J. & Tang, Y. 2010 Formation of aligned ZnO nanotube arrays by chemical etching and coupling with CdSe for photovoltaic application. *Thin Solid Films* **518**, 5146–5152.

Ma, S., Li, R., Lv, Ch., Xu, W. & Gou, X. 2011 Facile synthesis of ZnO nanorod arrays and hierarchical nanostructures for photocatalysis and gas sensor applications. *Journal of Hazardous Materials* **192**, 730–740.

Quintana, M., Ricra, E., Rodríguez, J. & Estrada, W. 2002 Spray pyrolysis deposited zinc oxide films for photo-electrocatalytic degradation of methyl orange: influence of the pH. *Catalysis Today* **76**, 141–148.

Quintana, M., Rodríguez, J., Solis, J. & Estrada, W. 2005 The influence of the ethanol-water molar ratio in the precursor solution on morphology and photocatalytic activity of pyrolytic ZnO films. *Photochemistry and Photobiology* **81**, 783–788.

Rodríguez, J., Paraguay-Delgado, F., López, A., Alarcón, J. & Estrada, W. 2010 Synthesis and characterization of ZnO nanorod films for photocatalytic disinfection of contaminated water. *Thin Solid Films* **519**, 729–735.

Rodríguez, J., Sánchez, L., Onna, D., Claudia Marchi, M., Ponce, S., Candal, R. & Bilmes, S. A. 2013 The role of seeding in the structure and wettability of ZnO nanorods films. *Applied Surface Science* **279**, 197–2013.

Talebian, N., Amininezhad, S. M. & Doudi, M. 2013 Controllable synthesis of ZnO nanoparticles and their morphology-dependent antibacterial and optical properties. *Journal of Photochemistry and Photobiology B: Biology* **120**, 66–73.

Wang, G., Da, Ch., Hao, Z., Jin, Z. & Jinghong, Li. 2008 Tunable photocurrent spectrum in well-oriented zinc oxide nanorod arrays with enhanced photocatalytic activity. *Journal of Physical Chemistry C* **112**, 8850–8855.

Wang, Xi, Meiyong, L., Yeteng, Z., Jian, Y., Wei, T., Tianyou, Z. & Chunyi, Z. 2012 ZnO hollow spheres with double-yolk egg structure for high-performance photocatalysts and photodetectors. *Advanced Materials* **24**, 3421–3425.

Wang, Z. L. 2004 Nanostructures of zinc oxide. *Materials Today* **7**, 26–33.

Yi, S., Choi, S., Jang, J., Kim, J. & Jung, W. 2007 Low-temperature growth of ZnO nanorods by chemical bath deposition. *Journal of Colloid and Interface Science* **313**, 705–710.

First received 10 December 2013; accepted in revised form 16 June 2014. Available online 30 June 2014